Engineering Transactions, **73**(4): 579–590, 2025, https://doi.org/10.24423/engtrans.3522.2025
Institute of Fundamental Technological Research Polish Academy of Sciences (IPPT PAN)
Université de Lorraine • Poznan University of Technology

Research Paper

Determination of Operating Conditions of a Probe Block Designed for Fault Diagnostics in Rail Heads

Zbigniew RANACHOWSKI[1)*], Sławomir MACKIEWICZ[1)], Tomasz KATZ[1)], Tomasz DĘBOWSKI[1)], Grzegorz STARZYŃSKI[1)], Marcin LEWANDOWSKI[1)], Łukasz ANTOLIK[2)]

[1)] *Institute of Fundamental Technological Research Polish Academy of Sciences*
Warsaw, Poland

[2)] *Railway Research Institute*
Warsaw, Poland

[*]Corresponding Author e-mail: zranach@ippt.pan.pl

In this paper, the key parameters influencing the proper operation of ultrasonic probes for railway rails diagnostics are determined. The goal is to test a set of ultrasonic probes under conditions occurring at high diagnostic speeds. Four issues are studied in more detail. The probe block-rail contact force required to obtain maximum echo level is determined. In the authors' opinion, the key aspect is the design of the water irrigation nozzle shape in order to produce a laminar couplant flow under the probes. The dependence of the amplitude of the recorded echo on the coupling layer thickness is experimentally investigated. The population of registered signal samples is processed to determine the testing speed limit, which resulted from the loss of data validation ability. The speed limit is calculated based on the average value of the amplitude of the measured signal and the standard deviation of the registered population of amplitudes.

The conducted research allows the authors to conclude that the instrumentation they developed enables the recording of an ultrasonic signal propagating through the tested rail at scanning speed of up to 100 km/h.

Keywords: railway rail diagnostics; ultrasonic examination; ultrasonic probe-rail interface.

1. Introduction

Today's railway transport for both people and goods operates on most routes at speeds exceeding 100 km/h. To guarantee the safe operation of the traffic,

appropriate rail testing procedures that do not disrupt regular traffic are necessary. Zumpano and Meo [1] described worldwide rail line testing procedures that include several non-destructive techniques: visual (VT), ultrasonic (UT), eddy current (ET), and magnetic (MT) testing. In the European Union, the standard EN 16729-3 [2] applies in these procedures. Examples of instrumentations for rail testing designed in the USA and Germany were presented by Heckel *et al.* [3, 4]. In an extensive review on ultrasonic technology for rail testing [5], the authors stated that during investigations, there is a necessity to determine the size, nature and location of defects. Such tasks are impossible to achieve when applying a single test probe. In practice, up to ten probes per single rail are used simultaneously. The application of such a large number of heads requires housing them in resistant blocks. This problem is being addressed individually by railway companies. According to reports [6], the Polish asset owner, PKP Polskie Linie Kolejowe S.A. (PKP PLK; PKP Polish Railway Lines), performs the ultrasonic defectoscopy of the rails using equipment limited to an operating speed of 40 km/h. To overcome this serious impediment, PKP PLK, supported by the Polish National Centre for Research and Development, launched a research project titled "An innovative solution enabling the implementation of defectoscopic examinations of rails at speeds from 60 km/h to 120 km/h". The subject of the aforementioned project includes several aspect, including hardware, software, and methods for acquiring ultrasonic testing (UT) data. The following paper deals with optimizing the operational conditions of UT sensors.

To prevent wear of ultrasonic probes used for on-site rail diagnostics in harsh field environments, they are placed in special holders. These robust blocks of probes are designed to enable quick probe change, extend probe lifespan, and also minimize the necessary liquid couplant consumption required for ultrasonic inspection. The layout design of the arrangement of five probe blocks, mounted on a wagon trolley and pressed against the rail by a spring system is presented in Fig. 1. This layout design was prepared under the supervision of the authors

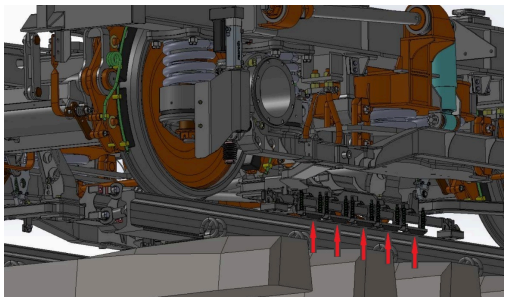

Fig. 1. Red arrows indicate the five ultrasonic probe blocks placed in a wagon trolley and pressed against the rail surface by a system of springs.

of the presented work as part of the ongoing research project conducted by the Polish National Centre for Research and Development and Polish Railway (see Acknowledgments).

Papers on nondestructive rail testing [3, 4] present various individual solutions of the implementation of probe blocks in operating diagnostic cars. Therefore, the aim of the authors of this paper was to design their own solution optimally adapted to local infrastructural requirements. To ensure effective fault detection, the following detailed parameters of the designed probe blocks were to be determined:

- probe block–rail pressing level,
- geometry of coupling liquid jet,
- thickness of the water coupling layer and its influence on the signal attenuation,
- maximum operational velocity of probe block to ensure an acceptable signal-to-noise ratio (SNR) during operation.

Theoretical calculations related to the operation of ultrasonic probes during rail testing were described by the authors in a wider study [7]. Friction of the probe block part against the rail during the movement of the probe block during its operation can cause an increase of its temperature. However, the contact pins shown in Fig. 5 can dissipate excess heat to the rail. The results of research on thermal processes during tread braking of railway wheels carried out on the brake torque dynamometer are presented in [8]. Moreover, it should be emphasized that the probe block described in presented paper is equipped with an irrigation system supplied by cold water. The authors of the article performed temperature measurements of the probe block under operational conditions. The irrigation system used made it possible to compensate for the effect of temperature increases in the probe block, associated with friction effects.

2. Instrumentation

Since the probe blocks are part of mobile diagnostic system, a special arrangement was prepared for laboratory testing of their capabilities. A brake torque dynamometer manufactured by ZF Group [9] was an essential part of this arrangement. The revolving shaft of the dynamometer was attached to a steel disc, which resulted in the relative movement of the block traveling across the surface of the disc. The probe block was guided on a disc by a holder equipped with adjustable pressing springs. The UT beam was generated by a 19 mm diameter transducer with a 3 MHz resonant frequency. The necessary water coupling system was also arranged using normal tap water. The details of the arrangement for testing the probe blocks are shown in Fig. 2.

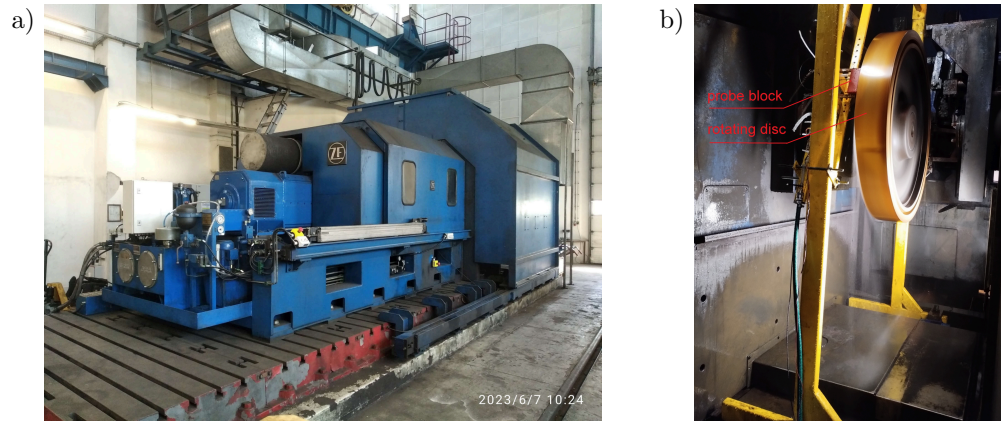

FIG. 2. Brake torque dynamometer manufactured by ZF Group used for testing the probe blocks (a); holder to fix the probe block onto the disk surface (b).

The disc thickness was of the same dimension as the rail head thickness to enable a simulation of the propagation of ultrasonic beam through the rail element. The UT beam was triggered at a repetition rate of 1100 Hz by a digital flaw detector, model EPOCH 650 [10]. The same defectoscope was applied for filtering and amplifying the received signal using the echo method. The details of the implemented materials testing method are described in the textbook by KRAUTKRÄMER and KRAUTKRÄMER [11]. The digital defectoscope processed the received signal in the following way. Analog-to-digital conversion was performed at a rate of 100 MHz with 10-bit resolution. A time-domain gate of 2 μs width was set in a way to extract from the ultrasonic echo the component representing the beam reflection from the rear side of the tested disk. The filtered echo component was latched to preserve its level until the next measuring sequence and then passed to the data acquisition system, prepared by applying the USB1901 module from ADLINK Technology [12]. In the established testing procedure, the received echo amplitude is displayed by the EPOCH defectoscope in decibels and, after adjusting the amplification, its level is stored for further processing as a percentage relative to the maximum set level, denoted as full scale height (FSH).

A preliminary test was performed to check the consistency of the prepared instrumentation. The probe block was placed with its face in direct contact with the rotating disk. Water coupling was implemented with a flow rate of 2.61 per minute (determined during initial checking). The disc's rotational speed was set in the manner to achieve a linear movement of 80 km/h, then the speed increased to 140 km/h. Inevitable vibrations and air "blasts" generated during the test caused the implemented water coupling between the ultrasonic probe and the disk to lose its effectiveness, as it is presented in Fig. 3. However, when the disc's

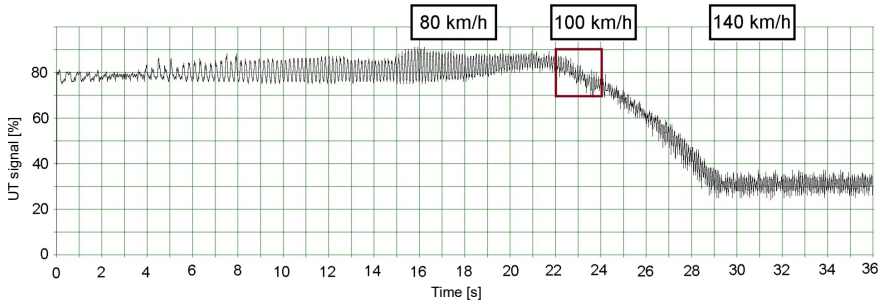

FIG. 3. Percentage level of the ultrasonic signal registered in the laboratory setup. The red square marks the moment (at the 23rd second of the test) when the movement speed of the probe block against the disk increased to 100 km/h.

rotational speed did not increase further, the amplitude of the registered signal remained stable.

3. Experimental results

3.1. Determining the optimal block pressure and irrigation nozzle shape

The authors conducted a number of tests in order to obtain a stable coupling layer when performing with the developed instrumentation. The high-speed movement of the probe block combined with a proper water coupling system results in a positive effect of aquaplaning, described in more detail by Vilsan and Sandu [13]. In our case, the movement-induced water pressure in front of the block forces a wedge under the front side of the block, forming a continuous liquid interface beneath the ultrasonic heads. This effect is highly desirable for the proper transmission of UT signal. However, excessive pressure applied to the probe block may result in breaking the liquid interface. Research was therefore undertaken to determine the proper spring pressing applied to the probe block to achieve the least value of UT wave attenuation caused by the interface. The results of this investigation are presented in Fig. 4. It is possible to draw the conclusion that applying a force of 16 N results in the most efficient conditions for UT wave transmission in the designed testing setup.

The water coupling nozzle geometry was the second parameter studied to improve the efficiency of probe block operation. A steady, laminar flow of the couplant from the nozzle implies uniform distribution of water across the lower surface of the block. Preliminary tests performed with the initial versions of the probe blocks revealed that simple circular terminations of the nozzle were ineffective and the couplant flow was not directed toward the UT sensor. Therefore, two other nozzle shapes were examined. A probe block prototype equipped

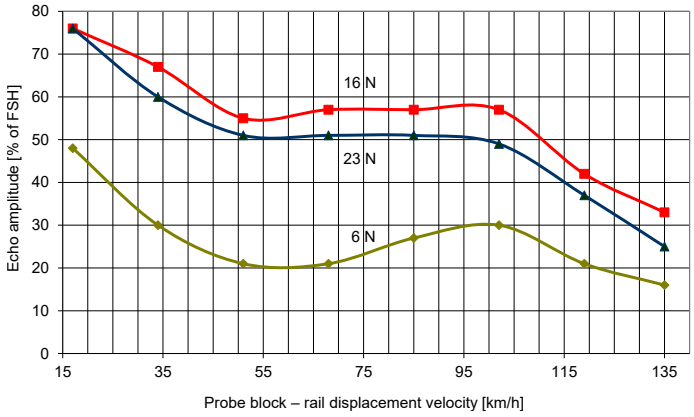

FIG. 4. Dependence of the received echo amplitude on the spring-applied pressure to the probe block recorded in the desired probe block-rail displacement velocity range.

with these nozzles is presented in Fig. 5. The triangular versus slot-like (square) nozzle shape efficiencies were compared, and the results are depicted in Fig. 6.

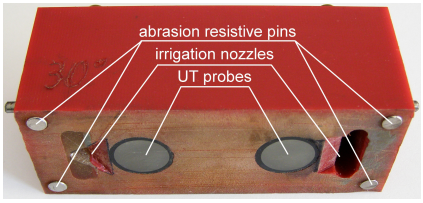

FIG. 5. Bottom view of the investigated probe block. There is the triangular irrigation nozzle on the left side of the block and the slot-like shaped one on the right side of the block. Two round UT probes are visible between the nozzles.

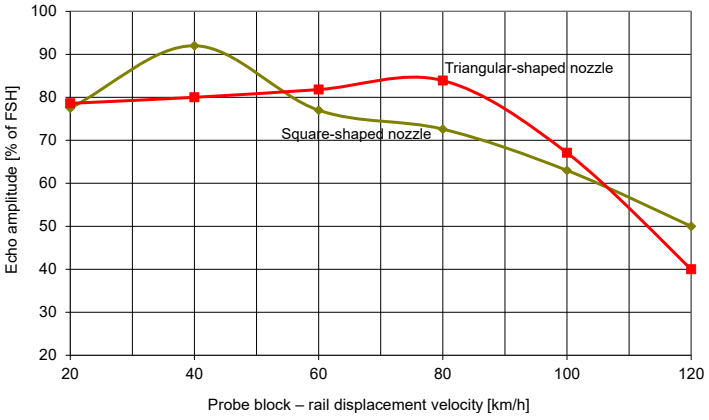

FIG. 6. Comparison of the efficiency of two irrigation nozzles, i.e., triangular- and square-shaped as couplant dispensers.

The conclusion resulting from this comparison is that the triangular-shaped nozzle delivered a higher UT echo amplitude during tests. An acceptable level of UT echo amplitude registered when applying irrigation with the triangular-shaped nozzle was confirmed to be within the speed range of up to 100 km/h.

3.2. Selection of optimal interface layer thickness

The quality of acoustic coupling between the probe and the tested rail is one of the key factors related to high-speed UT inspection of railway tracks. Under real testing conditions, the gap between the rail surface and the testing probes may vary due to surface waviness and dents. To minimize the resulting signal loss, the water coupling system must be carefully designed. The idea that the lower surface of the probe block and the surface of ultrasonic probes press directly against the wetted rail surface has proven impractical. HECKEL *et al.* [3] reports instead that high-speed rail inspection systems use probe blocks equipped with some abrasion-resistant pins to set the gap thickness d to 0.2 mm between the probes surface and the rail surface. This arrangement ensures better irrigation and extends the probe lifespan.

MACKIEWICZ *et al.* [7] provided a detailed determination of UT signal losses due to gap thickness variations. The authors modeled the transmission of an ultrasonic plane wave through a uniform liquid layer. The sources of the ultrasonic wave were a 0° normal probe and a 70° wedge probe. Coupling losses caused in the propagating beam by the presence of the layer were discussed and determined applying a numerical procedure. The problem was solved starting from the following assumptions.

Potential functions, for particle velocity φ_i for longitudinal waves (T-type) and ψ_i for transversal waves (L-type), were introduced. The explicit forms of these potential functions in the probe wedge, liquid layer, and rail material are as follows:

– in the probe wedge:

$$\varphi_1 = B_1 e^{-i(\propto_1 z - \sigma x)}, \qquad \psi_1 = D_1 e^{-i(\beta_1 z - \sigma x)}, \tag{3.1}$$

– in the liquid layer:

$$\varphi_2 = B_2 e^{-i(\propto_2 z - \sigma x)} + A_2 e^{i(\propto_2 z - \sigma x)}, \qquad \psi_2 = 0, \tag{3.2}$$

– in the rail material:

$$\varphi_3 = B_3 e^{-i(\propto_3 z - \sigma x)} + A_3 e^{i(\propto_3 z - \sigma x)}, \qquad \psi_3 = C_3 e^{i(\beta_3 z + \sigma x)}, \tag{3.3}$$

where α_i are the z-coordinates of the wave vectors for the longitudinal wave, β_i are the z-coordinates of the wave vectors for the transversal waves, A_i are the amplitudes of potential functions for L-type waves traveling in the positive z-direction, B_i are the amplitudes of potential functions for L-type waves traveling in the negative z-direction, C_i are the amplitudes of potential functions for T-type waves traveling in the positive z-direction, D_i are the amplitudes of potential functions for T-type waves traveling in the negative z-direction, and σ is the x-coordinate of all the wave vectors. The coordinates σ have to be equal to meet the continuity conditions at the interfaces.

Normal stresses and particle velocities due to the generated waves were then calculated by applying linear combinations of the potential functions presented above. Finally, Mackiewicz *et al.* [7] determined the transmission coefficients related to the ultrasonic wave propagating from the probe wedge to the tested material.

It is important that, for small gap thicknesses, a local maximum in these losses is observed at 0.2 mm for the typical wavelengths used in industrial defectoscopy. This suggests that if the gap d is set to 0.2 mm, unwanted changes in this setting in no case would degrade the echo amplitude. The theoretical coupling losses CL, presented in [7], for typical longitudinal and transverse wave probes as a function of d are depicted in Fig. 7.

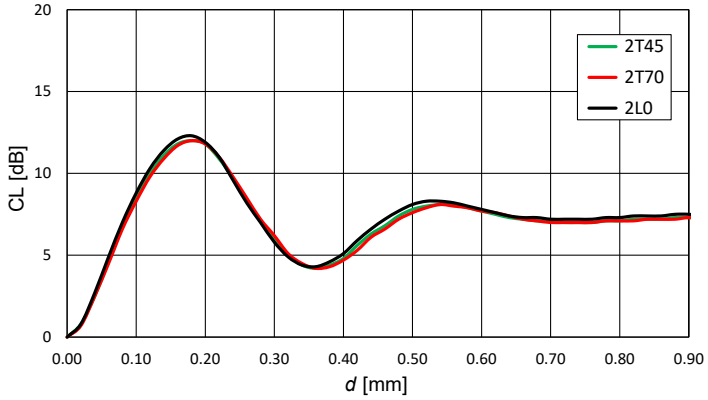

Fig. 7. Theoretical calculation of coupling loss characteristics CL for 2 MHz longitudinal wave (2L0), 2 MHz 70° transverse wave (2T70) and 2 MHz 45° transverse wave (2T45) probes as a function of gap thickness (after Mackiewicz *et al.* [7]).

Theoretical calculations match well the experimental results obtained from laboratory tests applying the brake torque dynamometer arrangement. These results are depicted in Fig. 8. It is obvious that the echo amplitude registered at $d = 0$ presents the highest level. Also, the losses observed at 0.2 mm gap d are higher than those registered at both 0.1 mm and 0.3 mm up to 100 km/h.

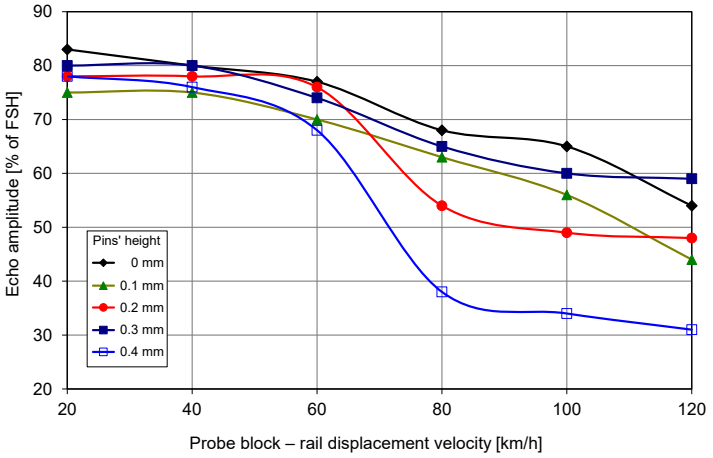

FIG. 8. Dependence of the received echo amplitude versus block-rail displacement velocity registered for various interface layer thickness, regulated by the distancing pins.

3.3. Problem of data validation

The ultrasonic echo resulting from the presence of a defect in the investigated rail volume is accompanied by unwanted electromagnetic noise generated by the registering system and environmental sources. The echo amplitude, in particular, depends on the temporary coupling quality and the accuracy of the block positioning. There is a parameter used in practical defectoscopy to validate the registered data in comparison to the present noise level. The determination of this parameter is similar to what is done in the image processing technique discussed by RUSS [14] and is known as SNR. The SNR is defined as the ratio of the mean signal μ calculated from a set of amplitude samples during the recording session to the standard deviation σ of that population of amplitudes:

$$\mathrm{SNR} = 20 \log (\mu/\sigma) \ [\mathrm{dB}]. \tag{3.4}$$

It is assumed that, to ensure the required quality of the registered data, μ has to exceed half of σ, that is, the value of SNR less than 13 dB is unacceptable. The assessment of SNR determined based on the described tests is presented in Fig. 9.

The set of determined SNR values led the authors to conclude that an interface layer established in the range of 0 mm–0.2 mm resulted in the acquisition of data at an acceptable level of the SNR parameter. However, the increase of the layer beyond 0.2 mm caused a critical decline in the registered data quality at displacement velocity higher than 80 km/h. The presence of numerous sources affecting, in practice, the quality of the registered UT echo let HECKEL *et al.* [3]

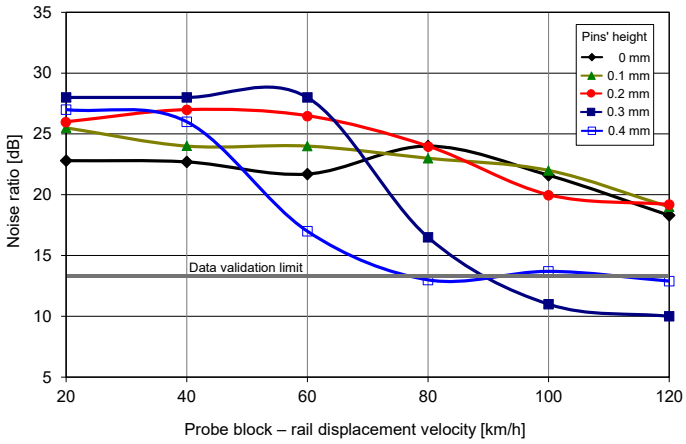

FIG. 9. Dependence of the determined SNR parameter from five tests performed at various interface layer thickness regulated by the distancing pins.

to state that the velocity of 80 km/h is close to the speed limit for mobile rail defectoscopy.

4. Conclusions

In this paper, the optimization of the operational conditions for a sensor block used in mobile defectoscopy of rails, was presented. The following aspects related to the design of this instrumentation were discussed:

- the research proved that to benefit from the aquaplaning effect, the pressing force applied to the tested sensor block should not exceed 16 N,
- to ensure laminar flow of the couplant, the application of a triangular irrigation nozzle proved to be most advantageous,
- experimental determination of the ultrasonic signal loss occurring at the probe-rail interface was performed. These results led the authors to recommend an optimal interface layer thickness of 0.2 mm,
- the assessment of SNR parameter determined as a function of probe-rail interface thickness at different probe block speeds enabled identifying conditions necessary for reliable data acquisition procedure.

All the presented findings led the authors to conclude that the described probe block design is capable of successful operation at speeds up to 100 km/h.

Acknowledgments

The paper was written as a part of research project no. BRIK II/0013/2022. The project was a joint undertaking of the Polish National Centre for Research

and Development and PKP PLK to support scientific research and development in the field of railway infrastructure, titled "Research and Development in Railway Infrastructure BRIK II".

References

1. Zumpano G., Meo M., A new damage detection technique based on wave propagation for rails, *International Journal of Solids and Structures*, **43**(5): 1023–1046, 2006, https://doi.org/10.1016/j.ijsolstr.2005.05.006.

2. Standard EN 16729-3, *Railway applications – Infrastructure – Non-destructive testing on rails in track – Part 3: Requirements for identifying internal and surface rail defects*, CEN, 2018.

3. Heckel T., Thomas H.M., Kreutzbruck M., Rühe S., High speed non-destructive rail testing with advanced ultrasound and Eddy-current testing techniques, [in:] *Proceedings of the National Seminar & Exhibition on Non-Destructive Evaluation*, pp. 261–265, 2009.

4. Heckel T., Casperson R., Rühe S., Mook G., Signal processing for non-destructive testing of railway tracks, [in:] *AIP Conference Proceedings*, **1949**(1): 030005, 2018, https://doi.org/10.1063/1.5031528.

5. Xue Z., Xu Y., Hu M., Li S., Systematic review: Ultrasonic technology for detecting rail defects, *Construction and Building Materials*, **368**: 130409, 2023, https://doi.org/10.1016/j.conbuildmat.2023.130409.

6. PKP Polskie Linie Kolejowe S.A., *Continuous track diagnostics for train traffic safety* [in Polish: *Stała diagnostyka torów dla bezpieczeństwa ruchu pociągów*], 2022, https://www.plk-sa.pl/o-spolce/biuro-prasowe/informacje-prasowe/szczegoly/stala-diagnostyka-torow-dla-bezpieczenstwa-ruchu-pociagow-6641 (access: 2025.05.23).

7. Mackiewicz S., Ranachowski Z., Katz T., Dębowski T., Starzyński G., Ranachowski P., Modeling of acoustic coupling of ultrasonic probes for high-speed rail track inspection, *Archives of Acoustics*, **49**(2): 255–266, 2024, https://doi.org/10.24425/aoa.2024.148787.

8. Cuperus J.L., Venter G., On the convective heat transfer from railway wheels, [in:] *Proceedings of the 11th International Heavy Haul Association Conference* (*IHHA 2027*), pp. 1029–1035, 2017.

9. ZF Group, Test systems for brakes, n.d., https://www.zf.com/products/en/testsystems/anwendungen/test_systems_for_brakes/test_systems_for_brakes.html (access: 2025.05.23).

10. EVIDENT, Ultrasonic flaw detectors, n.d., https://ims.evidentscientific.com/en/flaw-detectors/ultrasonic.

11. Krautkrämer J., Krautkrämer H.J., *Ultrasonic Testing of Materials*, 4 ed., Springer, Berlin, Heidelberg, 1990, https://doi.org/10.1007/978-3-662-10680-8.

12. ADLINK Technology, USB DAQ. USB-1901/1902/1903. 8/16-CH 16-Bit 250 kS/s multifunction USB DAQ modules (OEM version available), n.d., https://www.adlinktech.com/Products/Data_Acquisition/USBDAQ/USB-1901_1902_1903.

13. Vilsan A., Sandu C., Hydroplaning of tires: A review of numerical modeling and novel sensing methods, *Journal of Autonomous Vehicles and Systems*, **3**(3): 031001, 2024, https://doi.org/10.1115/1.4065379.

14. Russ J.C., *The Image Processing Handbook*, 5th ed., CRC Press, Boca Raton FL, London, New York, 2007.

Received February 18, 2025; accepted version July 31, 2025.
Online first October 17, 2025.